The SWI/SNF KlSnf2 Subunit Controls the Glucose Signaling Pathway To Coordinate Glycolysis and Glucose Transport in Kluyveromyces lactis

Pascale Cotton, Alexandre Soulard, Micheline Wésolowski-Louvel, Marc Lemaire

EC
Journals.ASM.org

The SWI/SNF KlSnf2 Subunit Controls the Glucose Signaling Pathway To Coordinate Glycolysis and Glucose Transport in *Kluyveromyces lactis*

Pascale Cotton, Alexandre Soulard, Micheline Wésolowski-Louvel, and Marc Lemaire

Génétique Moléculaire des Levures, UMR5240 Microbiologie, Adaptation et Pathogénie, Université de Lyon, Lyon, France; Université Lyon1, Lyon, France; and CNRS, Villeurbanne, France

In *Kluyveromyces lactis*, the expression of the major glucose permease gene *RAG1* is controlled by extracellular glucose through a signaling cascade similar to the *Saccharomyces cerevisiae* Snf3/Rgt2/Rgt1 pathway. We have identified a key component of the *K. lactis* glucose signaling pathway by characterizing a new mutation, *rag20-1*, which impairs the regulation of *RAG1* and hexokinase *RAG5* genes by glucose. Functional complementation of the *rag20-1* mutation identified the *KlSNF2* gene, which encodes a protein 59% identical to *S. cerevisiae* Snf2, the major subunit of the SWI/SNF chromatin remodeling complex. Reverse transcription-quantitative PCR and chromatin immunoprecipitation analyses confirmed that the KlSnf2 protein binds to *RAG1* and *RAG5* promoters and promotes the recruitment of the basic helix-loop-helix Sck1 activator. Besides this transcriptional effect, KlSnf2 is also implicated in the glucose signaling pathway by controlling Sms1 and KlRgt1 posttranscriptional modifications. When KlSnf2 is absent, Sms1 is not degraded in the presence of glucose, leading to constitutive *RAG1* gene repression by KlRgt1. Our work points out the crucial role played by KlSnf2 in the regulation of glucose transport and metabolism in *K. lactis*, notably, by suggesting a link between chromatin remodeling and the glucose signaling pathway.

Glucose is a signaling nutrient that drives cell growth and development through complex intracellular networks. Adaptation of cells to their environment involves sophisticated mechanisms for sensing glucose availability and responding appropriately through sugar signaling processes. Learning how plants, animals, and microorganisms respond to glucose is of great interest in understanding how they adapt to their environment. Moreover, deregulation of glucose sensing, uptake, and metabolism impacts the lifestyles of cells and organs and is correlated to pathologies and disorders like obesity, cancer, and diabetes (27, 28, 45). In the field of infection, induction of a metabolic environment conducive to human cytomegalovirus and hepatitis C viruses (HCV) implies drastic changes to the host cell metabolic network, notably, by increasing glucose import and glycolytic flux. Thus, HCV initially reprograms the cell to favor increased glucose fermentation and the partitioning of glycolytic intermediates toward the synthesis of cellular metabolites supporting the viral life cycle (12, 29). In fungi, sugar sensing influences yeast-hypha morphogenesis and biofilm formation in *Candida albicans*, which is essential for host colonization and optimal virulence (4, 40).

The environmental glucose sensing and signal transduction pathway has been accurately investigated in the model yeast *Saccharomyces cerevisiae* (22, 41). However, the respiratory aerobic yeast *Kluyveromyces lactis* provides a useful alternative model in which fermentation is facultative, a lifestyle more typical of eukaryotic organisms than the *S. cerevisiae* fermentative metabolism. Moreover, unlike *S. cerevisiae*, *K. lactis* displays little if any redundancy in the genes involved in glucose metabolism (14, 55). *K. lactis* has a simplified glucose uptake system that relies on two genes, *HGT1* and *RAG1*, encoding a high-affinity (2) and a low-affinity (8) permease, respectively. The *RAG1* permease gene, induced by high glucose concentrations, is necessary for supporting fermentative growth, which requires a high flow of substrate. In the absence of Rag1, *K. lactis* cells become respiration dependent for growth on high-glucose medium, and *rag1* mutants are unable to grow on 5% glucose when respiration is blocked by antimycin A (Rag^- phenotype) (8, 51).

Several *RAG* genes controlling the expression of *RAG1* have been identified in *K. lactis* and implicated in several pathways (Fig. 1). In the absence of glucose, the repressor KlRgt1, associated with the regulatory Sms1 factor (Std1/Mth1 orthologue), represses *RAG1* gene expression (20, 39). The presence of extracellular glucose is detected by the membrane Rag4 sensor (1), which, in cooperation with the Rag8 casein kinase I (3), generates an intracellular signal. This glucose signal induces Sms1 degradation through the SCF^{KlGrr1} complex and the subsequent phosphorylation-induced inactivation of the repressor KlRgt1 (20). Once derepressed, *RAG1* expression is further activated by the Sck1 glycolytic transcriptional activator (24, 33). KlRgt1 also represses the expression of hexokinase *RAG5* and *SCK1* genes (39). On the other hand, Rag8 kinase phosphorylates Sck1 and controls its stability, but independently of glucose availability (33). Importantly, an intracellular signal generated by glycolysis is also necessary for the glucose induction of *RAG1* gene expression in *K. lactis* (25).

To establish the connections between the different pathways in *K. lactis*, it is necessary to study glucose signal transduction in more detail. For this purpose, the study of new *rag* mutations that affect *RAG1* expression is a powerful tool to identify new participants. In this work, we characterized the new *rag20-1* allele and

Received 30 July 2012 **Accepted** 13 September 2012
Published ahead of print 21 September 2012
Address correspondence to Pascale Cotton, pascale.cotton@univ-lyon1.fr.

doi:10.1128/EC.00210-12

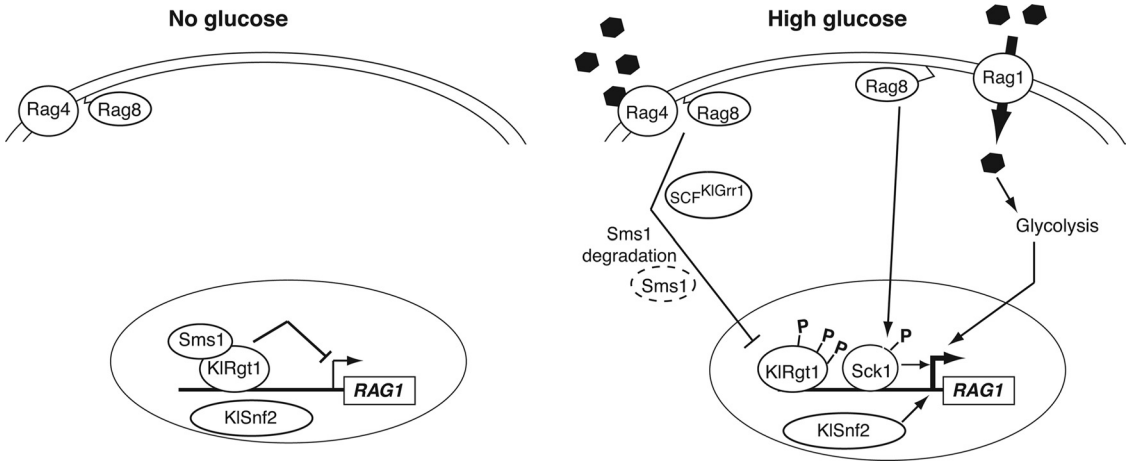

FIG 1 Simplified model for regulatory networks controlling *RAG1* gene expression in response to glucose availability. Phosphorylation events (P) on KlRgt1 and Sck1 are indicated. The role of KlSnf2 is detailed in this study. Rag1, low-affinity glucose permease; KlRgt1, transcriptional repressor; Sms1, KlRgt1-associated corepressor; Rag4, membrane glucose sensor; Rag8, membrane-associated casein kinase I; KlGrr1, F-box subunit of SCF complex; Sck1, bHLH transcriptional activator.

identified the corresponding *KlSNF2* gene as a key element for both the glucose signaling pathway and glucose metabolism regulation in *K. lactis*.

MATERIALS AND METHODS

Yeast strains and growth conditions. The yeast strains used in this study are listed in Table 1. Yeast cells were grown at 28°C in complete yeast extract-peptose (YP) medium containing 1% Bacto yeast extract, 1% Bacto peptone (Difco, Detroit), supplemented with either 2% glucose (YPG) or a specified carbon source. Minimal medium containing 0.7% yeast nitrogen base without amino acids (Difco) and 2% glucose was supplemented with auxotrophic requirements. The Rag phenotype was tested on GAA medium (YP containing 5% glucose and 5 μM antimycin A). For G418 medium, YPG plates were supplemented with Geneticin (200 μg/ml; Life Technologies).

Standard yeast genetic manipulations were performed as described previously (49, 50). *KlSNF2* epitope tagging and deletion of *KlSNF2*, *KlSWI1*, and *KlSNF5* genes were performed using a PCR-based strategy (26) in a Δ*Klnej1* genetic context, which facilitated gene targeting by homologous recombination in *K. lactis* (50). *KlSNF2*, *KlSWI1*, and *KlSNF5* deletions were performed in a Δ*Klnej1*/Δ*Klnej1* diploid, followed by meiosis analysis. The *KlSNF2* gene was inactivated with a 1.7-kb Δ*Klsnf2*::*URA3* cassette, resulting from NotI-BglII digestion of the pGD4 plasmid (see Table 2), and Ura$^-$ cells (KLPC09) were counterselected by plating strain KLPC05-10A on medium containing 5-fluoroorotic acid (5-FOA).

Cloning and plasmid constructions. The plasmids used are listed in Table 2. The *KlSNF2* gene was cloned by *in vivo* complementation of the Rag$^-$ phenotype displayed by the *rag20-1* mutant (PM6-7A/VV78) by using a genomic DNA library of *K. lactis* made in the centromeric *URA3* KCp491 vector (37). Among 7,000 Ura$^+$ transformants, 1 displayed a Rag$^+$ phenotype and carried a plasmid (pGD78 [Table 2]) with a 7-kb insert. The identification and positioning of *KlSNF2* in the inset was achieved by sequencing. A 3-kb NheI-PvuII fragment containing the *KLSNF2* gene from pGD78 (Table 2) was cloned into pBluescript KS(+), yielding the pGD3 plasmid. The Δ*Klsnf2*::*URA3* cassette was constructed by replacing the *KlSNF2* 1-kb HindIII internal fragment with the *URA3* marker in pGD3, yielding plasmid pGD4.

RNA extraction and RT-qPCR analysis. Total RNA extraction was performed as previously described (39). For reverse transcription-quantitative PCR (RT-qPCR) experiments, 10 μg of total RNA extract was

TABLE 1 *K. lactis* strains used in this study

Strain	Relevant genotype	Source or reference
MW270-7B	*MAT***a** *uraA1-1 leu2 metA1-1*	2
PM6-7A	*MAT***a** *uraA1-1 adeT-600*	8
MWL9S1	*MAT***a** *uraA1-1 leu2 lysA1-1 trp1 metA1-1* Δ*Klnej1*::*loxP*	50
MW392-3A	*MAT*α *uraA1-1 trp1 hisA2* Δ*Klnej1*::*LEU2*	Lab collection
MWK7	Isogenic to MW270-7B except *Klrgt1*Δ*1*::*URA3*	39
MLK2	Isogenic to MW270-7B except Δ*sck1*::*LEU2*	24
MLK209	Isogenic to MWL9S1 except *SMS1-3HA*::*kanMX6*	Lab collection
MWLK1099	Isogenic to MWL9S1 except *RGT1-3HA*::*kanMX6*	Lab collection
PM6-7A/VV78	*MAT***a** *uraA1-1 adeT-600 rag20-1(Klsnf2-1)*	This study
KLPC10	Isogenic to PM6-7A/VV78 except *RGT1-3HA*::*kanMX6*	This study
KLPC02	Isogenic to MWL9S1 except *KlSNF2-3HA*::*kanMX6*	This study
KLPC05-10A	*MAT*α *trp1 metA1 hisA2* Δ*Klsnf2*::*URA3*	This study
KLPC09	Isogenic to KLPC05-10A except Δ*Klsnf2*::*ura3*	This study
MW368-3C	*MAT*α *uraA1-1 leu2 Klrgt1*Δ*1*::*URA3 Klsnf2-1*	This study
MLK281	*MAT*α *uraA1-1 leu2 trp1 metA1-1* Δ*Klnej1*::*loxP* Δ*Klsnf2*::*URA3 SMS1-3HA*::*kanMX6*	This study
KLPC08	*MAT*α *uraA1-1* Δ*sck1*::*LEU2 KlSNF2-3HA*::*kanMX6*	This study

TABLE 2 Plasmids used in this study

Plasmid	Characteristics	Source or reference
pCXJ10	*K. lactis URA3-Klori*, multicopy vector	7
pCXJ22	*S. cerevisiae*/*K. lactis URA3* shuttle multicopy vector	7
pGD78	KCp491 carrying *KlSNF2*	This study
pGD3	pBluescript KS(+) carrying *KlSNF2*	This study
pGD4	pBluescript KS(+) carrying Δ*Klsnf2*::*URA3*	This study
pML219	pCXJ22 carrying *KlSNF2-3HA*	This study
pHN19	pCXJ10 carrying *LexA-SCK1*	Lab collection

treated with DNase I (Ambion), and the absence of DNA was confirmed by PCR with *Taq* DNA polymerase (Lucigen). DNase I-treated RNA extracts were then treated with SuperScript III reverse transcriptase (Invitrogen) as described by the manufacturer. RT-qPCR experiments were performed with the CFX 96 Bio-Rad light cycler using SYBR green I master mix (Roche). Relative quantification was based on the $2^{\Delta CT}$ method using *KlACT1* (actin) as calibrator. The amplification reaction conditions were as follows: 95°C for 5 min, and 40 cycles of 95°C for 10 s, 58°C for 10s, and 72°C for 30 s. *RAG1*, *RAG5*, and *KlACT1* amplifications were performed using the P548 (5′-TTTCTGGTTTAGGTGTTGGT-3′)/P549 (5′-CTTAAATGTTTAGGAGCGGTTT-3′), P550 (5′-GTGCTTACTAC GATGTTG-3′)/P551 (5′-AGGAACCATATTCACAGT-3′), and P547 (5′-ACATCAACATCACACTTC-3′)/P546 (5′-AACTGCTTCTCAATCA TC-3′) primers couples, respectively.

ChIP analysis. Chromatin immunoprecipitation (ChIP) experiments were performed as previously reported (33). *RAG1* and *RAG5* promoters were amplified using P250 (5′-TCGTCTGGAGTTCTTCGTCTG-3′)/ P269 (5′-AGACTAATGGCCGAGATACCG-3′) and P585 (5′-CTTCTT CCACAAAGTTCCTT-3′)/P586 (5′-GGTATACAATTCACAGTGG-3′) primer couples, respectively. The *KlTHI4* promoter (used as a control) was amplified with P301 (5′-TCTTTCCCGTTTACTCTCGA-3′) and P302 (5′-GCATTCCATACCATATTACT-3′).

Yeast cell extracts and immunoblotting. Cells were grown to mid-exponential phase in YPG, or in YP medium supplemented with 2% glycerol, or in selective media for cells containing the appropriate plasmid. Protein extracts were prepared according to the methods described by Kushnirov (23). Immunodetection conditions were as previously described (39).

RESULTS

The *RAG20* gene is the orthologue of the *S. cerevisiae SNF2* gene. Previous genetic analyses showed that the *rag20* mutant (PM6-7A/VV78 [Table 1]) of our laboratory Rag$^-$ mutant collection carries a monogenic recessive mutation, *rag20-1*, and belongs to a distinct complementation group (data not shown). The corresponding *RAG20* gene was cloned by functional complementation of the *rag20-1* mutation (see Materials and Methods), leading to the isolation of 7-kb complementing genomic DNA fragment carried by pGD78 (Table 2). Sequence analysis and BLAST comparison to the annotated *K. lactis* genome (14) revealed the presence in the pGD78 insert of a unique open reading frame (ORF), *KLLA0B08327g* (NCBI gene ID 2897166), which is similar to the *SNF2* gene of *S. cerevisiae*. We constructed a *rag20* null mutant (KLPC05-10A [Table 1]) which displayed a Rag$^-$ phenotype and a growth defect on glucose medium similar to that observed with the *rag20-1* mutant (Fig. 2B). The *rag20* null mutation was not complemented by the *rag20-1* mutation, as crossing these two mutant strains led to a diploid showing a Rag$^-$ phenotype (data not shown). Moreover, the *rag20-1* allele mutation in the PM6-7A/VV78 strain was identified by PCR amplification and sequencing. This allele carries two mutations in codons 1000 and 1001, leading to I1000N and W1001R substitutions in the Rag20-1 protein sequence (Fig. 2A). Altogether, these results demonstrated that the *RAG20* gene corresponds indeed to the cloned *KLLA0B08327g* ORF.

The *RAG20* gene encodes a 1,534-amino-acid-long protein that shares similar features with Snf2 of *S. cerevisiae* (Fig. 2A), which belongs to a large family of helicase-related proteins (17). In *S. cerevisiae* and many eukaryotes, Snf2 is the catalytic subunit of ATP-dependent chromatin remodeling complexes (SWI/SNF)

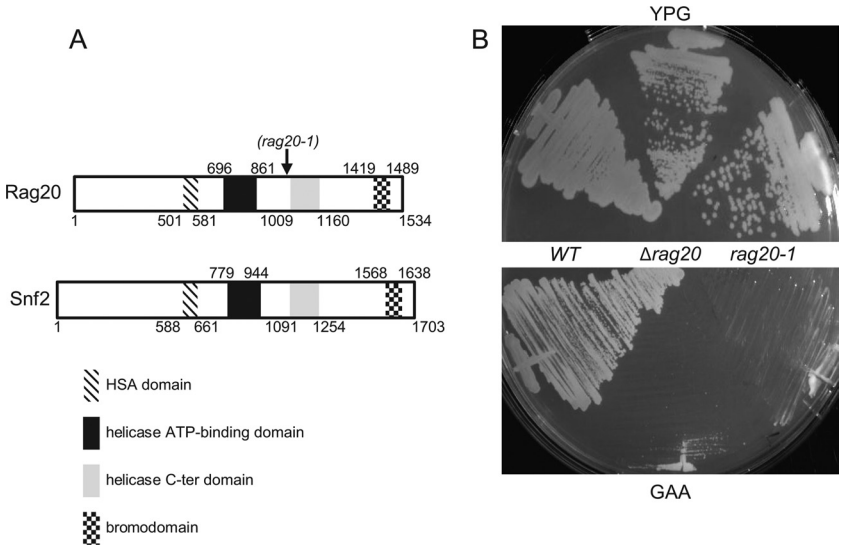

FIG 2 *RAG20* encodes a chromatin remodeling factor homologous to *S. cerevisiae* Snf2. (A) Schematic representations of Rag20 (*K. lactis*) and Snf2 (*S. cerevisiae*). Conserved domains found in Snf2-type enzymes are indicated by boxes with various types of shading. Numbers below or above the boxes indicate their position within the amino acid sequences. Mutations in the *rag20-1* allele positioned at amino acids 1000 and 1001 are indicated by an arrow. (B) Rag phenotypes of the mutants *rag20-1* (PM67-A/VV78) and Δ*rag20* (KLPC05-10A). Strains were streaked on YPG plates and GAA plates. The WT strain (MW270-7B) was used as a control. The photographs were taken after 2 days of incubation at 28°C.

that regulate the structure and dynamic properties of chromatin (9). The Rag20 protein harbors several conserved domains in Snf2-like proteins (Fig. 2A): a DNA binding domain (a helicase SANT-associated [HSA] domain) (13); a central ATPase domain composed of an ATP-binding domain, required for binding and hydrolysis of ATP, and a terminal helicase domain that may play a role in energy transduction (42); a C-terminal bromodomain known to interact with acetylated lysines of histones (54). Localizations and lengths of the Rag20 conserved domains strictly paralleled the *S. cerevisiae* Snf2 conserved domains (Fig. 2A). Protein sequence alignment showed that Rag20 is 59% identical to *S. cerevisiae* Snf2, and this identity reached 85% between the ATPase domains. Interestingly, the I1000N and W1001R substitutions lying within the ATPase domain of the Rag20-1 protein, upstream of the terminal helicase domain (Fig. 2A), are likely to gravely impact the enzyme three-dimensional structure (15, 44). These structural similarities strongly suggest that *RAG20* and *S. cerevisiae SNF2* genes are orthologues. This hypothesis is also corroborated by the conservation of synteny found at the *RAG20/SNF2* loci between these two yeast species (5). With regard to Snf2 similarity, we renamed the *RAG20* gene and the *rag20-1* mutation *KlSNF2* and *Klsnf2-1*, respectively.

In *S. cerevisiae*, SWI/SNF is a 12-subunit complex that is not essential for viability, despite the broad range of cellular processes that depend on it (6). Like Snf2, Snf5 and Swi1 subunits are implicated in chromatin remodeling, directly contacting acidic activators (38), and are also crucial for SWI/SNF complex integrity (36). To confirm the implication of the SWI/SNF complex in *RAG1* gene regulation, we attempted to inactivate putative SWI/SNF subunit genes in *K. lactis* and check their Rag phenotype. A brief survey of the *K. lactis* genome (www.genolevures.org/) identified the *KLLA0E18767g* and *KLLA0D12232g* ORFs as *SNF5* and *SWI1* homologues, respectively. However, the deletion of both genes by the *KanMX4* marker in a diploid strain and subsequent meiosis analysis led to only two G418-sensitive spores in all tetrads, showing that the putative *KlSNF5* and *KlSWI1* genes are essential for *K. lactis* viability.

***KlSNF2* is involved in the glucose regulation of *RAG1* permease and *RAG5* hexokinase gene expression.** Genetic analysis of Rag$^-$ mutants (52) led to the identification of *trans*-acting factors involved in *RAG1* regulation. As *Klsnf2* mutant strains showed a Rag$^-$ phenotype and a growth defect on glucose-containing medium, we investigated if the *KlSNF2* gene product could positively regulate the *RAG1* permease gene. The Δ*Klsnf2* and *Klsnf2-1* mutants were grown in the presence or absence of glucose, and *RAG1* mRNA steady-state levels were analyzed by RT-qPCR (Fig. 3A). In comparison to the parental wild-type (WT) strain, *RAG1* expression was severely affected in the *Klsnf2-1* and Δ*Klsnf2* mutants grown on glucose (3.4- and 7-fold, respectively), suggesting that KlSnf2 is required for glucose induction of *RAG1* gene expression. However, we previously showed that *RAG1* expression is also dependent on functional glycolysis, as its glucose induction is blocked in hexokinase *rag5* or enolase *Kleno* mutants (25). To check for such a putative indirect effect, we also examined the hexokinase *RAG5* gene expression level in the *rag20* mutants (Fig. 3B). The levels of *RAG5* mRNA were also severely decreased in the Δ*Klsnf2* and *Klsnf2-1* mutants grown in the presence of glucose (8- and 3-fold, respectively). Altogether, our data showed that KlSnf2 is involved in the glucose induction of *RAG1* and *RAG5* transcription and raised the question of whether the role of KlSnf2 in *RAG1* expression is direct or not.

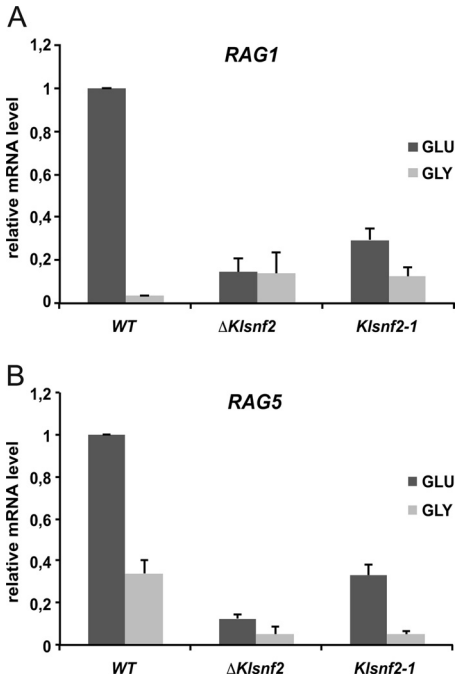

FIG 3 Transcriptional analysis of *RAG1* (A) and *RAG5* (B) in *Klsnf2* mutants. Levels of mRNA transcripts were determined in wild-type strain MW270-7B (WT), Δ*Klsnf2* (KLPC05-10A), and the *Klsnf2-1* mutant (PM6-7A/VV78). Cells were grown in the presence of glucose (GLU) or glycerol (GLY). Levels were normalized to the *ACT1* transcript level. In total, three biological replicates were performed. Standard errors originated from RT-qPCR replicates. For each strain, mRNA levels are shown relative to the level of *RAG1* (A) or *RAG5* (B) transcripts in the WT strain grown in the presence of glucose, which was set to 1.

KlSnf2 is present on *RAG1* and *RAG5* promoters *in vivo*. In *S. cerevisiae*, the SWI/SNF ATP-dependent chromatin remodeling complex is recruited to targeted promoters for activation and repression of a subset of genes (36). To test for a direct role of KlSnf2 in *RAG1* and *RAG5* expression, we investigated the interaction of KlSnf2 with *RAG1* and *RAG5* promoters in ChIP assays. To immunoprecipitate KlSnf2, we first constructed the KLPC02 strain (Table 1), where KlSnf2 was epitope tagged by genetic recombination at the *KlSNF2* gene. The resulting KlSnf2-3HA fusion (HA represents hemagglutinin) was expressed and found to be functional, since the KLPC02 strain displayed a Rag$^+$ phenotype (data not shown). ChIP experiments were carried out in *KlSNF2-3HA* or untagged *KlSNF2* cells. After immunoprecipitation, we used the IP and total input DNA (IN) for PCR analysis with primers designed for *RAG1* and *RAG5* promoters (p*RAG1* and p*RAG5*). Figure 4A shows that sequences of p*RAG1* and p*RAG5* were specifically enriched in KlSnf2-3HA IP fractions of cells grown in the presence of glucose. These results suggest that KlSnf2 interacts with *RAG1* and *RAG5* promoters to positively regulate these genes when glucose is present. However, the presence of KlSnf2 was also detected on the *RAG1* promoter when cells were grown in the absence of glucose (Fig. 4B), suggesting that this interaction is independent of glucose availability. As a control, promoter sequences of the *K. lactis THI4* gene, involved in thiamine biosynthesis, were not detected in IP fractions. These results emphasize

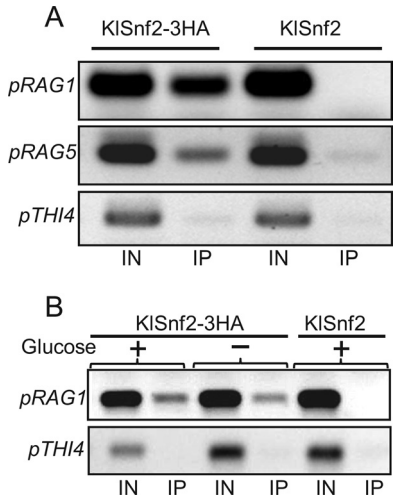

FIG 4 KlSnf2 is present on *RAG1* and *RAG5* promoters *in vivo*. (A) Binding of KlSnf2 to *RAG1* and *RAG5* promoters. Chromatin from glucose-grown cells expressing KlSnf2-3HA (KLPC02) or untagged KlSnf2 (MWL9S1) was extracted and immunoprecipitated with anti-HA antibodies. PCR was performed on total extracted (IN) or immunoprecipitated (IP) chromatin by using primers binding to the *pRAG1*, *pRAG5*, or *pTHI4* promoters. (B) KlSnf2 presence on the *pRAG1* promoter is not regulated by glucose. KLPC02 cells expressing KlSnf2-3HA were grown in 2% glucose (+) or 2% glycerol (−), and ChIP analysis was performed as described in the text. PCR products were resolved by electrophoresis in a 1.5% agarose gel and visualized by ethidium bromide staining. ChIP experiments were done in triplicate, and representative results are shown.

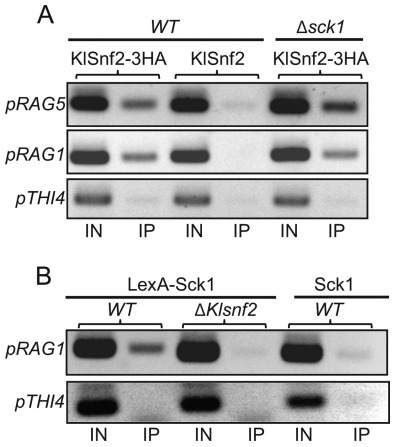

FIG 5 KlSnf2 and Sck1 interplay on the *RAG1* promoter. (A) KlSnf2 binds to the *RAG1* and *RAG5* promoters in the absence of Sck1. *SCK1* (WT; KLPC02) and Δ*sck1* (KLPC08) cells expressing KlSnf2-3HA were grown on 2% glucose, and extracted chromatin was immunoprecipitated using anti-HA antibody. MWL9S1 cells expressing untagged KlSnf2 were used as a control. (B) LexA-Sck1 binding to the *RAG1* promoter is dependent on KlSnf2. PM67A (WT) and KLPC09 (Δ*Klsnf2*) cells expressing LexA-Sck1 (pHN19 plasmid) were grown on 2% glucose. PM67A cells carrying pCXJ10 (empty vector) were used as a control. Chromatin was extracted and immunoprecipitated using anti-LexA antibodies. ChIP analyses were conducted as described in the legend for Fig. 4, here using a set of primers that bind to the *RAG1*, *RAG5*, and *THI4* (used as a control) promoters. ChIP experiments were performed in triplicate. Representative results are shown.

our previous findings that glucose transport and glycolysis are coordinated at the transcriptional level in *K. lactis* not only by the interplay of the KlRgt1 repressor and Sck1 (33, 39), but also by the role of KlSnf2.

KlSnf2 binds to the *RAG1* promoter *in vivo* and promotes Sck1 recruitment. Snf2-like proteins interact with DNA with a low specificity, and SWI/SNF complexes are recruited to specific promoters through direct interactions with gene-specific activators (38, 56). In muscle cells, the basic helix-loop-helix (bHLH) myogenic MyoD activator interacts with the SWI/SNF subunit to target this complex to muscle-specific genes, enabling their transcriptional activation during muscle cell differentiation (11). As both the bHLH Sck1 activator and KlSnf2 are directly involved in glucose induction of the *RAG1* and *RAG5* genes in *K. lactis*, we asked whether the recruitment of KlSnf2 on these promoters could be dependent on Sck1 activator. We first constructed a Δ*sck1 KlSNF2-HA* strain (KLPC08 [Table 1]) by genetic crosses and tetrads dissection. ChIP assays were then conducted by immunoprecipitating KlSnf2-3HA from *SCK1 KlSNF2-HA* (KlPC02) and Δ*sck1 KlSNF2-HA* (KLPC08) cells grown in the presence of glucose. Figure 5A shows that sequences from p*RAG1* and p*RAG5* were enriched to the same extent in KlSnf2-3HA IP fractions from cells either expressing Sck1 or not. These results demonstrated that KlSnf2 is recruited to *RAG1* and *RAG5* promoters independently of Sck1 activator.

SWI/SNF recruitment and subsequent nucleosome rearrangement induce a local chromatin open state suitable for recruitment of gene-specific transcription factors on targeted promoters (6), and we wondered if the recruitment of the Sck1 activator to the *RAG1* promoter was dependent on the presence of KlSnf2. For that purpose, ChIP experiments were conducted in glucose-grown WT and Δ*Klsnf2* cells (KLPC09) transformed with the pHN19 plasmid (Table 2), expressing a functional LexA-Sck1 fusion (33), or with an empty vector. After immunoprecipitation with anti-LexA antibodies, sequences from the *RAG1* promoter were enriched in the IP fraction from WT cells (Fig. 5B), confirming that Sck1 is present *in vivo* on the *RAG1* promoter as previously described (33). However, this enrichment was strongly decreased in the IP fraction from Δ*Klsnf2* cells, suggesting that Sck1 was no longer efficiently associated with the *RAG1* promoter in the absence of KlSnf2.

Altogether, these data clearly show that the bHLH Sck1 activator is not required for KlSnf2 to be recruited to the *RAG1* promoter. On the other hand, the chromatin rearrangement presumably imposed by the presence of KlSnf2 on the *RAG1* promoter may facilitate the binding of Sck1 to optimize *RAG1* activation in glucose-grown cells.

Involvement of KlSnf2 in the Rag4 glucose signaling pathway. Glucose regulation of the *RAG1* gene strongly depends on the KlRgt1 repressor, which binds the *RAG1* promoter and represses its expression in the absence of glucose (39). In glucose-grown cells, Rag4 (glucose sensor) and Rag8 (casein kinase I) initiate a signaling pathway to target and inactivate KlRgt1 by phosphorylation (20). As KlSnf2 is directly involved in *RAG1* regulation, we investigated whether KlSnf2 could interfere or interact with the Rag4 glucose signaling pathway.

Previous studies demonstrated epistatic relationships between the *KlRGT1* and *RAG4/RAG8* genes, as the loss of KlRgt1 restored a Rag$^+$ phenotype and a high level of *RAG1* expression in *rag4* and *rag8* mutants (39). We first looked at genetic interactions between *KlRGT1* and *KlSNF2* by constructing a Δ*Klrgt1 Klsnf2-1* double mutant (MW368-3C [Table 1]). Figure 6A shows that the Δ*Klrgt1 Klsnf2-1* mutant displayed a Rag$^+$ phenotype, indicating that the

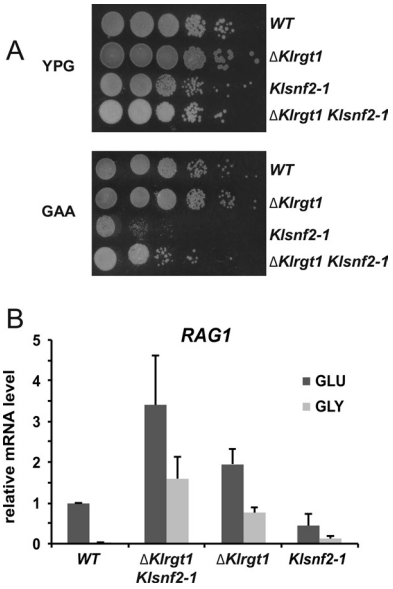

FIG 6 Rag20 and KlRgt1 genetically interact. (A) *KlRGT1* deletion suppresses the *KlSnf2-1* mutation. Strains were cultured on YPG medium to stationary phase, and cultures were then diluted to an optical density at 600 nm of 1. Constant amounts of serial dilutions were spotted either on YPG or GAA medium. The WT strain (MW270-7B) was used as a control. The photographs were taken after 2 days of incubation at 28°C. (B) Transcriptional analysis of *RAG1* in *Klrgt1* and *KlSnf2* mutants. Levels of mRNA transcripts were determined in wild-type strain MW270-7B (WT), Δ*Klrgt1 Klsnf2-1* (MW368-3C), Δ*Klrgt1* (MWK7), and *Klsnf2-1* mutant (PM6-7A/VV78). Cells were grown in the presence of glucose (GLU) or glycerol (GLY). Levels were normalized to the *ACT1* transcript level. In total, three biological replicates were performed. Standard errors originated from RT-qPCR replicates. For each strain, mRNA levels are presented relative to the level of *RAG1* transcript in the WT strain grown in the presence of glucose, which was set to 1.

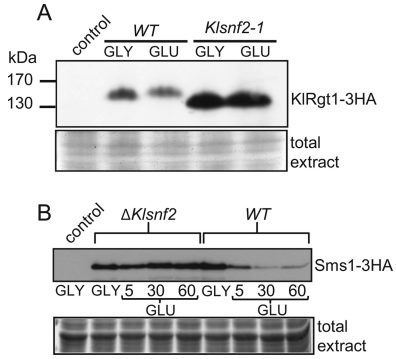

FIG 7 Rag20 is implicated in the glucose signaling pathway. (A) KlRgt1 is not phosphorylated in the presence of glucose in the Δ*Klsnf2* mutant. *Klsnf2-1* (KLPC10) and WT cells (MWLK1099) expressing KlRgt1-3HA were pregrown in YP glycerol to an optical density of 1, diluted 10 times in YP glycerol, and then transferred in YP glycerol supplemented with 2% glucose or 2% glycerol for 30 min. KlRgt1-3HA was detected by Western blotting using anti-HA antibodies. Total protein extracts were also used in parallel as loading controls. (B) Sms1 is not degraded in the presence of glucose in Δ*Klsnf2*. Sms1-3HA expressed in WT cells (MLK209) and Δ*Klsnf2* cells (MLK281) was detected by Western blotting after cells were grown in YP medium with 2% glycerol and transferred to YP 2% glycerol or YP 2% glucose for 5, 30, and 60 min. MWL9S1 cells expressing untagged KlRgt1 and Sms1 were used as a control in both panels. Total protein extracts were used in parallel as loading controls. Experiments were performed in triplicate. Representative results are shown.

KlRGT1 deletion (Rag^+) indeed suppressed the Rag^- phenotype of the *Klsnf2-1* mutant. We then analyzed by RT-qPCR the expression levels of the *RAG1* gene in Δ*Klrgt1*, *Klsnf2-1*, and Δ*Klrgt1 Klsnf2-1* mutants (Fig. 6B). As previously shown (39), the *RAG1* gene was not repressed in Δ*Klrgt1* cells grown in glycerol medium, and its expression was higher in glucose-grown cells than in the WT strain. On the other hand, *RAG1* was poorly expressed in the *Klsnf2-1* mutant, confirming that KlRgt1 and KlSnf2 have opposite effects on glucose regulation of the *RAG1* gene. In Δ*Klrgt1 Klsnf2-1* cells, *RAG1* expression was not repressed in glycerol-grown cells and was restored to high levels under glucose growth conditions (Fig. 6B). A similar behavior was also observed for the *RAG5* gene (data not shown). Altogether, these results suggested that *KlRGT1* and *KlSNF2* genetically interact and certainly cooperate to accurately regulate the *RAG1* gene in response to glucose availability. They are consistent with a model where KlSnf2 acts positively downstream of KlRgt1 in order to derepress *RAG1* once the repressor is inactivated. However, compared to Δ*Klrgt1* cells, *RAG1* expression was surprisingly enhanced in the Δ*Klrgt1 Klsnf2-1* strain when grown either in the presence or absence of glucose, suggesting a negative role for KlSnf2 in a context devoid of the KlRgt1 repressor. Interestingly, glucose induction of *RAG1* expression could still be observed in the Δ*Klrgt1* and Δ*Klrgt1 Klsnf2-1* mutants, presumably because of the Sck1 activator (or at least another unidentified activator) still present in these strains.

In addition to Sck1, KlSnf2 is the only known positive regulator interacting with *RAG1* promoter. Interestingly, *SCK1* gene deletion leads to a modest decrease of *RAG1* expression in the presence of glucose (24) while Δ*Klsnf2* null mutant harbors a drastic reduced level of *RAG1* glucose induction (Fig. 3A). This reduced level is similar to the situation found in the *rag4* and *rag8* mutants (1, 3), where KlRgt1 is not inactivated and *RAG1* expression is still repressed under glucose growth conditions (20, 39). This observation suggested additional roles for KlSnf2 in *RAG1* regulation and prompted us to check the KlRgt1 phosphorylation status in the *Klsnf2-1* mutant. Phosphorylated KlRgt1 displays a reduced electrophoretic mobility on SDS-PAGE (39). We first constructed the KLPC10 strain (Table 1) by crossing and meiosis analysis, showing that the previously described functional KlRgt1-3HA fusion was expressed (39). KLPC10 and WT strains (MWLK1099 [Table 1]) were grown either in the presence or the absence of glucose, and KlRgt1 phosphorylation status was investigated by Western blot analysis of total protein cell extracts (Fig. 7A). The presented results clearly showed the typical KlRgt1 mobility shift between glycerol- and glucose-grown cells of the WT strain, indicating KlRgt1 phosphorylation in response to glucose (39). In contrast, in the *Klsnf2-1* mutant, KlRgt1 exhibited a lower mobility independently of glucose availability, suggesting that KlRgt1 is not phosphorylated in glucose-grown *Klsnf2-1* cells. Interestingly, KlRgt1 mobility was even lower in the *Klsnf2-1* mutant than in WT glycerol-grown cells, suggesting additional missing posttranslational modifications in the *Klsnf2-1* mutant. Moreover, this lower-mobility form of KlRgt1 was more abundant in the *Klsnf2-1* mutant than in the WT strain, suggesting that this lower-mobility form either displays a greater *in vivo* stability or is more efficiently immunodetected. Altogether, these data show that KlSnf2 is required for KlRgt1 to be phosphorylated and inactivated in response to glucose.

Previous data showed that Sms1 regulates KlRgt1 activity by preventing its phosphorylation in the absence of glucose. Sms1 is

rapidly degraded in glucose-grown cells, and its degradation requires the glucose signal initiated by the Rag4 signaling pathway (20). Thus, we examined Sms1 steady-state level in the *Klsnf2-1* mutant after cells were shifted from glycerol to glucose (Fig. 7B). We used WT and *Klsnf2-1* cells expressing Sms1-3HA (MLK209 and MLK281 [Table 1]). Sms1 was rapidly degraded in glucose-grown WT cells, as previously described (20), whereas Sms1 depletion did not occur in *Klsnf2-1* mutant. Whatever the underlying mechanism, these results demonstrate that KlSnf2 influences glucose signaling by controlling Sms1 degradation and the consequent phosphorylation-induced KlRgt1 inactivation.

DISCUSSION

Glucose signaling is conserved between *K. lactis* and *S. cerevisiae*, and the general structure of the Snf3/Rgt2/Rag4 signaling pathway, which senses extracellular glucose, is very similar between the two yeasts (20, 30). The novel *KlSNF2*, homologous to the *SNF2* gene of *S. cerevisiae*, appears as a key element of the glucose signaling pathway in *K. lactis*, confirming that this aerobic yeast is a powerful model, and an alternative to *S. cerevisiae*, for discovering new elements of glucose signaling in yeasts. The *SNF2* gene was originally isolated in *S. cerevisiae* from an *snf* (sucrose-nonfermenting) genetic screen, and its product, Snf2, is required for the derepression of the invertase *SUC2* gene in the absence of glucose (32). Despite the involvement of several chromatin remodeling complexes, such as Ssn6-Tup1 and SAGA complexes, in the regulation of *HXT* hexose permease genes in *S. cerevisiae* (35, 46, 47), the roles of Snf2 and the SWI/SNF complex in *HXT* gene regulation still remains to be demonstrated. Rgt1 represses *HXT1* expression in the absence of glucose by recruiting the Ssn6-Tup1 complex (34, 46), which imposes a repressive chromatin structure in conjunction with histone deacetylases (16, 56). Interestingly, Ssn6-Tup1 and SWI/SNF complexes have antagonist remodeling effects in *S. cerevisiae* (18). As both *SSN6* and *TUP1* homologous genes are conserved in the *K. lactis* genome, further analysis will be necessary to determine their putative involvement in *RAG1* gene regulation.

ChIP analysis showed that KlSnf2 is associated with the *RAG1* and *RAG5* promoters, suggesting the recruitment of the *K. lactis* SWI/SNF complex to regulate *RAG1* and *RAG5* genes. Genome-wide expression analyses revealed that transcription of roughly 5% of *S. cerevisiae* genes requires the SWI/SNF complex, whose transcriptional role is exerted at the level of specific promoters rather than over a large chromosomal area (21, 43). The SWI/SNF complex can be recruited to targeted promoters via interactions either with RNA polymerase II holoenzyme (38) or with sequence-specific transcription activators. In *S. cerevisiae*, SWI/SNF is recruited to the *HO* promoter *in vivo* or to an artificial Gal4-driven promoter *in vitro* by the transcriptional Swi5 and Gal4 activators, respectively (10, 56). In muscle cells, SWI/SNF is targeted to specific promoters by the myogenic bHLH MyoD activator (11). To date, the bHLH Sck1 protein is the only transcriptional activator known to bind the *RAG1* promoter to specific UAS sequences (E-boxes) located in the −1150/−944 region (33). However, our results demonstrated that Sck1 does not trigger KlSnf2 recruitment to the *RAG1* promoter (Fig. 5B), which was in agreement with the difference between the moderate and severe *RAG1* expression levels observed in the Δ*sck1* (24) and Δ*Klnf2* (Fig. 3A) mutants. Interestingly, the loss of a *cis*-acting element in the *RAG1* promoter (−750/−621 region devoid of E-boxes) led to a drastic 20-fold decrease in expression of a *RAG1-lacZ* fusion (8). It remains unclear whether this promoter region binds an unidentified transcription factor, but we speculate that this additional activator may recruit the SWI/SNF complex to activate *RAG1* expression. On the other hand, nucleosome occupancy within a promoter influences accessibility of specific transcription factor binding motifs and modulates targeted gene expression in response to environmental nutrient variations (57). In the present study, we did not investigate nucleosome occupancy at the *RAG1* and *RAG5* promoters in response to glucose, but our results clearly show that KlSnf2 facilitates binding of the Sck1 activator to the *RAG1* promoter.

Recently, another mechanism has been proposed that links glucose metabolism to chromatin remodeling (19, 48). Histone acetylation, necessary for Snf2-mediated chromatin remodeling, relies on (ATP)-citrate lyase (ACL), which converts glucose-derived citrate into acetyl coenzyme A (CoA). Consequently, histone acetylation is regulated in a nutrient-dependent manner that relies on glucose and acetate availability. Glucose feeding causes a transient increase in acetylation, which contributes to transcriptional activation (19, 48). In *K. lactis*, glucose induction of the *RAG1* gene requires functional glycolysis (25), suggesting the existence of a metabolic intracellular signal in addition to the Rag4 pathway. The underlying mechanism is still unknown, but the glycolytic defect may cause acetyl-CoA depletion *in vivo* and could disturb histone acetylation at the *RAG1* promoter. In this context, it will be interesting to investigate whether hexokinase *rag5* or enolase *Kleno* mutants display a histone acetylation pattern suitable to KlSnf2 targeting to the *RAG1* promoter.

Glucose transport and glycolysis are tightly coordinated at the transcriptional level in *K. lactis*, and KlSnf2 appears as a major element of this metabolic coordination. KlRgt1 strongly locks glucose catabolism by repressing *RAG1* glucose permease gene and the hexokinase *RAG5* gene in the absence of glucose (39). This negative control is reinforced through KlRgt1 repression of the *SCK1* gene, whose product participates in activation of *RAG1* and glycolytic genes by glucose (20, 33). Once KlRgt1 is inactivated by the Rag4 signaling pathway, the presence of KlSnf2 on both *RAG1* and *RAG5* promoters could establish favorable conditions by generating a local chromatin topology conducive to transcription activation by the Sck1 activator. Second, hexokinase *RAG5* gene expression is severely impacted in the absence of KlSnf2. Hence, KlSnf2 exerts additional control on glucose uptake by controlling the glycolysis-mediated intracellular signal necessary for *RAG1* expression (25).

Finally, a significant insight gained from our study is that KlSnf2 is also implicated in the posttranslational regulation of KlRgt1 by controlling Sms1 degradation in the presence of glucose (Fig. 7B), but the underlying mechanism is still unclear. Sms1 degradation is triggered by the Rag4-dependent extracellular glucose signaling pathway (Fig. 1), which may be deficient in *Klsnf2* mutants. However, several pieces of evidence have indicated that this signaling pathway and its components (Rag4, Rag8, and KlGrr1) are still functional in the absence of KlSnf2. First, KlSnf2 and KlRgt1 do not presumably regulate the *RAG4* gene, since its expression is constitutive and not regulated by glucose (1). Second, in addition to a Rag$^-$ phenotype, the loss of KlGrr1 leads to an abnormal elongated cell morphology phenotype (20) which is not displayed by *Klsnf2* mutants (data not shown). Third, Rag8 kinase phosphorylates Sck1 to control its cellular steady-state

level, and a LexA-Sck1 fusion was degraded in a *rag8* mutant (33). However, during our ChIP experiments, we confirmed that LexA-Sck1 was expressed in the Δ*Klsnf2* mutant by Western blotting (data not shown), indicating that *KlSNF2* deletion has little if any effect on Rag8 kinase activity. On the other hand, considering the strong impact of KlSnf2 on expression of the *RAG5* hexokinase gene and other glycolytic genes (data not shown), the influence of KlSnf2 on KlRgt1 and Sms1 posttranslational control may be a consequence of impaired glycolysis in *Klsnf2* mutants and thus absence of the intracellular glucose signal. Finally, a direct implication of KlSnf2 in Sms1 degradation control remains biologically relevant as, besides its transcriptional role, the human Snf2 counterpart, the BRG1 protein, interacts with the p53 tumor suppressor and promotes its polyubiquitination and degradation *in vivo* in a chromatin remodeling-independent context (31). Indeed, SWI/SNF complexes represent a novel link between chromatin remodeling and cell tumorigenesis, as mutations in the human Snf2 counterpart BRG1 protein have been identified in various cancers (53). Thus, it will be interesting to analyze in detail the molecular mechanism of KlSnf2 control on Sms1 degradation and to investigate whether important and evolutionarily conserved functions exist in Snf2-like proteins, in addition to their well-known chromatin remodeling activities.

ACKNOWLEDGMENTS

We are greatful to Claire Bärtschi and Julien Deffaud for technical assistance. We thank Gaelle Dieppois and Thierry Dulermo for their contribution to this work.

REFERENCES

1. **Betina S, Goffrini P, Ferrero I, Wésolowski-Louvel M.** 2001. *RAG4* gene encodes a glucose sensor in *Kluyveromyces lactis.* Genetics **158**:541–548.
2. **Billard P, et al.** 1996. Glucose uptake in *Kluyveromyces lactis*: role of the *HGT1* gene in glucose transport. J. Bacteriol. **178**:5860–5866.
3. **Blaisonneau J, Fukuhara H, Wésolowski-Louvel M.** 1997. The *Kluyveromyces lactis* equivalent of casein kinase I is required for the transcription of the gene encoding the low-affinity glucose permease. Mol. Gen. Genet. **253**:469–477.
4. **Bonhomme J, et al.** 2011. Contribution of the glycolytic flux and hypoxia adaptation to efficient biofilm formation by *Candida albicans.* Mol. Microbiol. **80**:995–1013.
5. **Byrne KP, Wolfe KH.** 2005. The Yeast Gene Order Browser: combining curated homology and syntenic context reveals gene fate in polyploid species. Genome Res. **15**:1456–1461.
6. **Cairns BR.** 2009. The logic of chromatin architecture and remodelling at promoters. Nature **461**:193–198.
7. **Chen XJ.** 1996. Low- and high-copy-number shuttle vectors for replication in the budding yeast *Kluyveromyces lactis.* Gene **172**:131–136.
8. **Chen XJ, Wésolowski-Louvel M, Fukuhara H.** 1992. Glucose transport in the yeast *Kluyveromyces lactis.* II. Transcriptional regulation of the glucose transporter gene *RAG1.* Mol. Gen. Genet. **233**:97–105.
9. **Clapier CR, Cairns BR.** 2009. The biology of chromatin remodeling complexes. Annu. Rev. Biochem. **78**:273–304.
10. **Cosma MP, Tanaka T, Nasmyth K.** 1999. Ordered recruitment of transcription and chromatin remodeling factors to a cell cycle- and developmentally regulated promoter. Cell **97**:299–311.
11. **de la Serna IL, et al.** 2005. MyoD targets chromatin remodeling complexes to the myogenin locus prior to forming a stable DNA-bound complex. Mol. Cell. Biol. **25**:3997–4009.
12. **Diamond DL, et al.** 2010. Temporal proteome and lipidome profiles reveal hepatitis C virus-associated reprogramming of hepatocellular metabolism and bioenergetics. PLoS Pathog. **6**:e1000719. doi:10.1371/journal.ppat.1000719.
13. **Doerks T, Copley RR, Schultz J, Ponting CP, Bork P.** 2002. Systematic identification of novel protein domain families associated with nuclear functions. Genome Res. **12**:47–56.
14. **Dujon B, et al.** 2004. Genome evolution in yeasts. Nature **430**:35–44.
15. **Dürr H, Körner C, Müller M, Hickmann V, Hopfner KP.** 2005. X-ray structures of the *Sulfolobus solfataricus* SWI2/SNF2 ATPase core and its complex with DNA. Cell **121**:363–373.
16. **Edmondson DG, Smith MM, Roth SY.** 1996. Repression domain of the yeast global repressor Tup1 interacts directly with histones H3 and H4. Genes Dev. **10**:1247–1259.
17. **Flaus A, Martin DM, Barton GJ, Owen-Hughes T.** 2006. Identification of multiple distinct Snf2 subfamilies with conserved structural motifs. Nucleic Acids Res. **34**:2887–2905.
18. **Fleming AB, Pennings S.** 2001. Antagonistic remodelling by Swi-Snf and Tup1-Ssn6 of an extensive chromatin region forms the background for *FLO1* gene regulation. EMBO J. **20**:5219–5231.
19. **Friis RM, et al.** 2009. A glycolytic burst drives glucose induction of global histone acetylation by picNuA4 and SAGA. Nucleic Acids Res. **37**:3969–3980.
20. **Hnatova M, Wesolowski-Louvel M, Dieppois G, Deffaud J, Lemaire M.** 2008. Characterization of *KlGRR1* and *SMS1* genes, two new elements of the glucose signaling pathway of *Kluyveromyces lactis.* Eukaryot. Cell **7**:1299–1308.
21. **Holstege FC, et al.** 1998. Dissecting the regulatory circuitry of a eukaryotic genome. Cell **95**:717–728.
22. **Johnston M, Kim JH.** 2005. Glucose as a hormone: receptor-mediated glucose sensing in the yeast *Saccharomyces cerevisiae.* Biochem. Soc. Trans. **33**:247–252.
23. **Kushnirov VV.** 2000. Rapid and reliable protein extraction from yeast. Yeast **16**:857–860.
24. **Lemaire M, Guyon A, Betina S, Wésolowski-Louvel M.** 2002. Regulation of glycolysis by casein kinase I (Rag8p) in *Kluyveromyces lactis* involves a DNA-binding protein, Sck1p, a homologue of Sgc1p of *Saccharomyces cerevisiae.* Curr. Genet. **40**:355–364.
25. **Lemaire M, Wésolowski-Louvel M.** 2004. Enolase and glycolytic flux play a role in the regulation of the glucose permease gene *RAG1* of *Kluyveromyces lactis.* Genetics **168**:723–731.
26. **Longtine MS, et al.** 1998. Additional modules for versatile and economical PCR-based gene deletion and modification in *Saccharomyces cerevisiae.* Yeast **14**:953–961.
27. **Macheda ML, Rogers S, Best JD.** 2005. Molecular and cellular regulation of glucose transporter (GLUT) proteins in cancer. J. Cell. Physiol. **202**:654–662.
28. **Mathupala SP, Rempel A, Pedersen PL.** 2001. Glucose catabolism in cancer cells: identification and characterization of a marked activation response of the type II hexokinase gene to hypoxic conditions. J. Biol. Chem. **276**:43407–43412.
29. **McArdle J, Moorman NJ, Munger J.** 2012. HCMV targets the metabolic stress response through activation of AMPK whose activity is important for viral replication. PLoS Pathog. **8**:e1002502. doi:10.1371/journal.ppat.1002502.
30. **Moriya H, Johnston M.** 2004. Glucose sensing and signaling in *Saccharomyces cerevisiae* through the Rgt2 glucose sensor and casein kinase I. Proc. Natl. Acad. Sci. U. S. A. **101**:1572–1577.
31. **Naidu SR, Love IM, Imbalzano AN, Grossman SR, Androphy EJ.** 2009. The SWI/SNF chromatin remodeling subunit BRG1 is a critical regulator of p53 necessary for proliferation of malignant cells. Oncogene **28**:2492–2501.
32. **Neigeborn L, Carlson M.** 1984. Genes affecting the regulation of *SUC2* gene expression by glucose repression in *Saccharomyces cerevisiae.* Genetics **108**:845–858.
33. **Neil H, Hnatova M, Wesolowski-Louvel M, Rycovska A, Lemaire M.** 2007. Sck1 activator coordinates glucose transport and glycolysis and is controlled by Rag8 casein kinase I in *Kluyveromyces lactis.* Mol. Microbiol. **63**:1537–1548.
34. **Ozcan S, Johnston M.** 1996. Two different repressors collaborate to restrict expression of the yeast glucose transporter genes *HXT2* and *HXT4* to low levels of glucose. Mol. Cell. Biol. **16**:5536–5545.
35. **Ozcan S, Johnston M.** 1999. Function and regulation of yeast hexose transporters. Microbiol. Mol. Biol. Rev. **63**:554–569.
36. **Peterson CL, Workman JL.** 2000. Promoter targeting and chromatin remodeling by the SWI/SNF complex. Curr. Opin. Genet. Dev. **10**:187–192.
37. **Prior C, Mamessier P, Fukuhara H, Chen XJ, Wésolowski-Louvel M.** 1993. The hexokinase gene is required for transcriptional regulation of the glucose transporter gene *RAG1* in *Kluyveromyces lactis.* Mol. Cell. Biol. **13**:3882–3889.

38. **Prochasson P, Neely KE, Hassan AH, Li B, Workman JL.** 2003. Targeting activity is required for SWI/SNF function in vivo and is accomplished through two partially redundant activator-interaction domains. Mol. Cell **12**:983–990.
39. **Rolland S, Hnatova M, Lemaire M, Leal-Sanchez J, Wesolowski-Louvel M.** 2006. Connection between the Rag4 glucose sensor and the KlRgt1 repressor in *Kluyveromyces lactis.* Genetics **174**:617–626.
40. **Sabina J, Brown V.** 2009. Glucose sensing network in *Candida albicans*: a sweet spot for fungal morphogenesis. Eukaryot. Cell **8**:1314–1320.
41. **Santangelo GM.** 2006. Glucose signaling in *Saccharomyces cerevisiae.* Microbiol. Mol. Biol. Rev. **70**:253–282.
42. **Smith CL, Peterson CL.** 2005. A conserved Swi2/Snf2 ATPase motif couples ATP hydrolysis to chromatin remodeling. Mol. Cell. Biol. **25**: 5880–5892.
43. **Sudarsanam P, Iyer VR, Brown PO, Winston F.** 2000. Whole-genome expression analysis of snf/swi mutants of *Saccharomyces cerevisiae.* Proc. Natl. Acad. Sci. U. S. A. **97**:3364–3369.
44. **Thomä NH, et al.** 2005. Structure of the SWI2/SNF2 chromatin-remodeling domain of eukaryotic Rad54. Nat. Struct. Mol. Biol. **12**:350–356.
45. **Thorens B.** 2008. Glucose sensing and the pathogenesis of obesity and type 2 diabetes. Int. J. Obes. (Lond.) **32**(Suppl 6):S62–S71.
46. **Tomas-Cobos L, Sanz P.** 2002. Active Snf1 protein kinase inhibits expression of the *Saccharomyces cerevisiae HXT1* glucose transporter gene. Biochem. J. **368**:657–663.
47. **van Oevelen CJC, van Teeffelen HAAM, van Werven FJ, Timmers HTM.** 2006. Snf1p-dependent Spt-Ada-Gcn5-acetyltransferase (SAGA) recruitment and chromatin remodeling activities on the *HXT2* and *HXT4* promoters. J. Biol. Chem. **281**:4523–4531.
48. **Wellen KE, et al.** 2009. ATP-citrate lyase links cellular metabolism to histone acetylation. Science **324**:1076–1080.
49. **Wésolowski M, Algeri A, Goffrini P, Fukuhara H.** 1982. Killer DNA plasmids of the yeast *Kluyveromyces lactis.* Curr. Genet. **5**:191–197.
50. **Wésolowski-Louvel M.** 2011. An efficient method to optimize *Kluyveromyces lactis* gene targeting. FEMS Yeast Res. **11**:509–513.
51. **Wésolowski-Louvel M, Goffrini P, Ferrero I, Fukuhara H.** 1992. Glucose transport in the yeast *Kluyveromyces lactis.* I. Properties of an inducible low-affinity glucose transporter gene. Mol. Gen. Genet. **233**:89–96.
52. **Wésolowski-Louvel M, Prior C, Bornecque D, Fukuhara H.** 1992. *rag*$^{-}$ mutations involved in glucose metabolism in yeast: isolation and genetic characterization. Yeast **8**:711–719.
53. **Wilson BG, Roberts CW.** 2011. SWI/SNF nucleosome remodellers and cancer. Nat. Rev. Cancer **11**:481–492.
54. **Winston F, Allis CD.** 1999. The bromodomain: a chromatin-targeting module? Nat. Struct. Biol. **6**:601–604.
55. **Wolfe KH, Shields DC.** 1997. Molecular evidence for an ancient duplication of the entire yeast genome. Nature **387**:708–713.
56. **Yudkovsky N, Logie C, Hahn S, Peterson CL.** 1999. Recruitment of the SWI/SNF chromatin remodeling complex by transcriptional activators. Genes Dev. **13**:2369–2374.
57. **Zawadzki KA, Morozov AV, Broach JR.** 2009. Chromatin-dependent transcription factor accessibility rather than nucleosome remodeling predominates during global transcriptional restructuring in *Saccharomyces cerevisiae.* Mol. Biol. Cell **20**:3503–3513.